

<https://doi.org/10.1038/s43247-024-01407-6>

Extreme hydrometeorological events induce abrupt and widespread freshwater temperature changes across the Pacific Northwest of North America

Check for updates

Stephen J. Déry¹ ✉, Eduardo G. Martins², Philip N. Owens¹ & Ellen L. Petticrew¹

The Pacific Northwest of North America experienced four extreme hydrometeorological events during 2021 including intense cold waves in mid-February and late December, the record-setting June heat dome, and catastrophic floods caused by two November atmospheric rivers. While the synoptic-scale patterns and terrestrial hydrological responses to these extreme events are well documented, scant information has been published on corresponding freshwater temperature responses. Here, we apply an observational database of hourly freshwater temperatures at 554 sites across the region to characterize their evolution during these four extreme hydrometeorological events. The two cold snaps and summer heat dome induced a general 1 °C decline and 2.7 °C increase, respectively, in water temperatures with subdued changes (+0.4 °C) during the mid-November floods. For 193 sites with long-term records, 478 daily maximum water temperatures were exceeded during the heat dome and 94 were surpassed during the flooding event, suggesting deleterious effects for water quality and aquatic species.

The Pacific Northwest of North America (PNWNA) experienced four disruptive and destructive extreme hydrometeorological events during 2021. These disruptions comprised periods of extreme air temperatures (low temperatures, LT or high temperatures, HT) and high river flows (HF). The early summer “heat dome” (Event 2: high temperatures or E2:HT) was one of the most extreme heat waves ever recorded globally^{1–3}. Thereafter in mid-November, catastrophic floods in southwestern British Columbia (BC), Canada, and northwestern Washington, United States (US) ensued from a pair of intense landfalling atmospheric rivers⁴ (E3:HF). In early and late 2021, two severe cold waves also yielded extreme conditions across the region. The February 2021 cold wave (E1:LT) propagated from northwestern Canada through the PNWNA and beyond ultimately leading to a historical cold snap and major power outages in Texas, US^{5,6}. A similar cold wave (E4:LT) affected the PNWNA during late December 2021 with major impacts on electricity consumption, transportation, and outdoor recreation⁷.

In addition to socio-economic impacts, such extreme hydro-meteorological events can influence many ecologic conditions including

freshwater temperatures^{8,9}. While multiple atmospheric, hydrological, topographical, and stream channel conditions control freshwater temperatures^{10–13}, surface air temperatures and river discharge often explain most of the variance in daily and weekly stream temperature fluctuations^{11,14}. Despite recent studies assessing freshwater temperature responses to heat waves^{8,9,15–17}, droughts¹⁸, and climate change^{13,14,19}, a dearth of information exists in the literature on river temperature responses to intense synoptic-scale events¹⁵ generating abrupt and extreme changes in air temperature and streamflow. This lack of information is particularly apparent for freshwater temperature responses during cold waves, land-falling atmospheric rivers, and flood events¹⁹, which represent three of the four events in this study.

The overarching objective of this study is to describe how freshwater temperatures (T_w) across the PNWNA responded to four extreme hydro-meteorological events in 2021. Specifically, we aim: (1) to assess whether freshwater temperatures and their changes were atypical during the four extreme hydrometeorological events; and (2) to describe spatio-temporal patterns in freshwater temperature responses to these events and their

¹Department of Geography, Earth and Environmental Sciences, University of Northern British Columbia, 3333 University Way, Prince George, BC V2N 4Z9, Canada. ²Department of Ecosystem Science and Management, University of Northern British Columbia, 3333 University Way, Prince George, BC V2N 4Z9, Canada. ✉e-mail: sdery@unbc.ca

including central tendencies, dispersion metrics, and extreme values, of freshwater temperatures for all events of interest.

Freshwater temperature changes during four extreme hydrometeorological events

Average water temperature changes during the two LT events showed weekly $\Delta T_w = -1.0^\circ\text{C}$ and -1.2°C during February and December 2021, respectively (Table 2). Water temperature changes were less pronounced in February as many rivers were already near 0°C relative to the December event. The early summer heat dome (E2:HT) induced an overall weekly $\Delta T_w = 2.7^\circ\text{C}$ across the study area with a maximum weekly change of 8.5°C in northeastern BC. Changes in 5-day water temperatures were less pronounced at $+0.4^\circ\text{C}$ overall during the mid-November floods (E3:HF). In all four cases, results from the Wilcoxon signed-rank test confirmed that overall water temperature changes were significantly different from zero (Table 2).

The interquartile range of 2.1°C and standard deviation of 1.5°C illustrate the greater dispersion of water temperature changes during E2:HT relative to the other three events (Table 2 and Supplementary Fig. 4). During cold waves, more ΔT_w values approached zero owing to the large number of sites (147 or 33.4% for E1:LT and 153 or 36.5% for E4:LT) that were within 2°C of the freezing mark. The distribution of water temperature changes remained narrow for E3:HF as this was a high flow rather than an air temperature extreme event.

Regional patterns in ΔT_w also emerged during the four extreme hydrometeorological events (Fig. 2). E1:LT and E4:LT driven by cold waves covering the PNWNA showed similar patterns in water temperature responses. More northern, alpine waterways in BC saw minimal changes in water temperatures due to near-freezing conditions and/or ice cover; meanwhile, coastal and more southern basins (e.g., BC's Lower Mainland, Oregon's Willamette Valley) observed greater decreases in water tempera-

ture. During E2:HT, lower elevation, inland waterways (e.g., BC's lower Nechako, Nicola and Okanagan basins) experienced the greatest increases in water temperatures, whereas alpine, coastal, and some regulated streams saw more moderate changes (with decreases in some cases owing to rapid snow and glacier melt and/or cool water releases from reservoirs). In contrast, there were minimal changes in water temperatures in areas affected by the pair of atmospheric rivers during E3:HF although more southern locations (e.g., in Oregon) experienced moderate rises.

For E1:LT, E3:HF, and E4:LT, median Spearman rank correlations (ρ_m) of paired time series of standardized hourly water temperatures were 0.27, 0.21 and 0.16, respectively, revealing modest levels of spatial synchrony (Table 1). In contrast, $\rho_m = 0.62$ during E2:HT indicated a more coherent and homogenous response of freshwater temperatures across the entire PNWNA to the early summer heat dome.

Maps of changes in the standard deviation in T_w from the 7-day or 5-day period prior to and during the four events show distinct patterns from changes in the mean, particularly for E1:LT and E4:LT (c.f. Fig. 3 with Fig. 2). During E1:LT, standard deviations in T_w generally declined in northern BC but increased in southwestern BC, northwestern Washington and Oregon. In response to the early summer heat dome (E2:HT), variability in hourly T_w rose markedly in northern and interior BC as T_w increased but declined in coastal regions. Minimal changes in 5-day and 7-day T_w standard deviations marked E3:HF and E4:LT, respectively.

Changes in 7-day or 5-day average water temperatures post-event reflect whether impacts persisted beyond the duration of the extreme hydrometeorological events (Supplementary Fig. 5). Domain average water temperature changes post E1:LT, E2:HT, and E4:LT were minimal at $\leq|0.2^\circ\text{C}|$, while an overall cooling of 1.2°C followed E3:HF. For E1:LT, some sites observed a cooling trend while other waterways in southwestern BC and western Oregon reported a warming trend. After E2:HT, water temperatures generally continued to rise at a more moderate rate in northern BC; conversely, southwestern BC, western Washington, and Oregon observed rapid declines in water temperatures. E3:HF was marked by T_w cooling across the entire PNWNA with the greatest decreases in Oregon.

Table 1 | Statistics of the weekly or 5-day freshwater temperatures (T_w) during four extreme hydrometeorological events across the PNWNA in 2021

Event	Min. ($^\circ\text{C}$)	Median ($^\circ\text{C}$)	Mean ($^\circ\text{C}$)	Max. ($^\circ\text{C}$)	SD ($^\circ\text{C}$)	IQR ($^\circ\text{C}$)	ρ_m	TS_m ($^\circ\text{C}^\circ\text{C}^{-1}$)
E1:LT	0.00	2.40	2.69	10.48	2.18	3.79	0.27	0.13
E2:HT	2.28	17.29	16.91	27.83	5.01	7.34	0.62	0.46
E3:HF	0.02	7.50	6.90	13.38	3.34	5.01	0.21	0.10
E4:LT	0.00	1.79	2.45	11.30	2.22	3.85	0.16	0.17

SD denotes standard deviation, IQR represents the interquartile range, ρ_m denotes the median Spearman rank cross correlation value of standardized time series of hourly water temperatures for all possible paired sites, and TS_m is the median thermal sensitivity across all sites.

Atypicality of freshwater temperature conditions during four extreme hydrometeorological events

Freshwater temperatures and their weekly changes during four extreme hydrometeorological events were placed into context with respect to the remainder of 2021 and longer-term data. Cold waves associated with E1:LT and E4:LT induced the coldest water temperatures and lowest spread amongst all sites in 2021 (Fig. 4). Conversely, the early summer heat dome (E2:HT) yielded the warmest water temperatures and largest spread across all sites in 2021 while E3:HF observed more typical water temperatures relative to the remainder of 2021. Weekly water temperature changes reached their maximum during E2:HT and a near minimum during E1:LT.

Table 2 | Statistics of the weekly or 5-day water temperature changes (ΔT_w) for four extreme hydrometeorological events across the PNWNA in 2021

Event	Min. ($^\circ\text{C}$)	Median ($^\circ\text{C}$)	Mean ($^\circ\text{C}$)	Max. ($^\circ\text{C}$)	SD ($^\circ\text{C}$)	IQR ($^\circ\text{C}$)	Shapiro-Wilk Test ^a	Wilcoxon Rank Sum Test ^b
E1:LT	-3.80	-0.70	-0.98	1.20	1.01	1.72	$W_{SW} = 0.93$ $p = 6.78 \times 10^{-13}$	$W_W = 109,543$ $p = 1.61 \times 10^{-8}$
E2:HT	-2.59	2.83	2.74	8.46	1.54	2.13	$W_{SW} = 0.99$ $p = 4.12 \times 10^{-4}$	$W_W = 80,716$ $p < 2.2 \times 10^{-16}$
E3:HF	-2.33	0.19	0.39	3.40	0.89	1.05	$W_{SW} = 0.97$ $p = 5.12 \times 10^{-8}$	$W_W = 81,081$ $p = 0.04$
E4:LT	-3.74	-1.16	-1.18	0.51	1.01	1.90	$W_{SW} = 0.90$ $p = 1.40 \times 10^{-15}$	$W_W = 100,445$ $p = 2.44 \times 10^{-9}$

SD denotes standard deviation, IQR represents the interquartile range, while W_{SW} and W_W are the test statistics of the Shapiro-Wilk⁴⁷ and paired samples Wilcoxon rank sum tests⁵⁸, respectively. ^aThe null hypothesis for the Shapiro-Wilk test is that the distribution of weekly (5-day) water temperature changes are normally distributed. When $p < 0.05$, the null hypothesis is rejected indicating the water temperature changes are not normally distributed. ^bThe null hypothesis for the Wilcoxon rank sum test is that the paired values of weekly (5-day) average water temperature prior to and during the four extreme hydrometeorological events are not significantly different. When $p < 0.05$, the null hypothesis is rejected indicating the weekly (5-day) water temperatures are significantly different prior to then during the events.

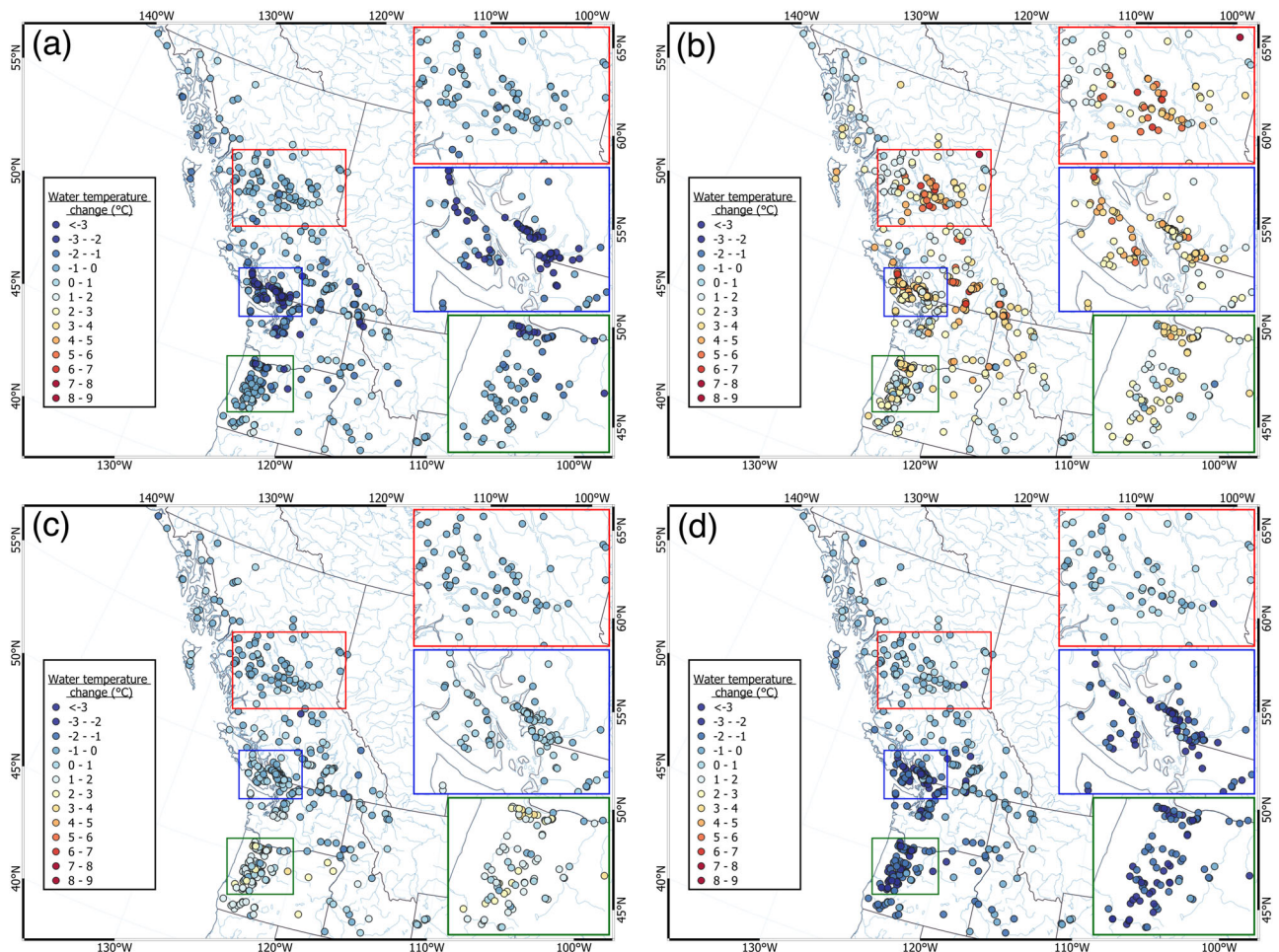


Fig. 2 | Weekly (5-day) changes in average hourly water temperatures during four extreme hydrometeorological events across the PNWNA in 2021. Results are shown for (a) E1:LT ($n = 423$), (b) E2:HT ($n = 492$), (c) E3:HF ($n = 420$), and (d) E4:LT ($n = 402$). Source data to create Fig. 2 are available in Supplementary Data 3.

Thus, thermal conditions during E1:LT, E2:HT, and E4:LT were generally atypical than the remainder of the year with more typical conditions in E3:HF. Although cooling episodes comparable to E1:LT and E4:LT unfolded in late summer 2021, the associated interquartile ranges showed subdued responses relative to the two cold waves.

The 193 sites with long-term (≥ 10 years) records revealed the unusual nature of the water temperatures experienced during the 2021 heat dome (E2:HT). In all, 478 daily maximum water temperature historical records were exceeded from 25 June to 1 July 2021, comprising 37.4% of the available measurements. Yet another 94 daily maximum water temperature historical records were surpassed on 11–15 November 2021 (E3:HF), equivalent to 18.4% of the available measurements. Daily minimum water temperature historical records were reached for 9.8% and 13.0% of the available measurements during E1:LT and E4:LT, respectively.

The most pronounced standardized departures from long-term means occurred during E2:HT and E4:LT (Fig. 5). During the early summer heat dome (E2:HT), clusters of standardized anomalies >2 appeared in the Willamette and Okanagan valleys, while lower values were reported in northern BC. In response to the late December cold wave (E4:LT), large (<-1.5) standardized anomalies emerged across the southern half of the study area. During E1:LT and E3:HF, standardized anomalies were generally $<|1.5|$, although the Willamette Valley experienced values >1.5 during the mid-November floods. Pearson cross correlations between absolute values of standardized departures from long-term means and record lengths were statistically significant ($r \geq 0.70$, $p < 0.05$) for all four events, suggesting

standardized departures were likely underestimated at sites with relatively shorter records.

Potential associations with terrestrial, hydrological, and meteorological conditions

Cross correlations between various terrestrial, hydrological, and meteorological conditions revealed seasonal dependencies with water temperature changes (Table 3). While mean basin elevation, catchment area, and longitude were not correlated to ΔT_w , latitude explained up to 34.6% of the variance during all four events. Average water temperature in the 7-day or 5-day period prior to the events and changes in weekly (5-day) T_{air} showed negative correlations with ΔT_w in E1:LT and E4:LT, but positive correlations during E2:HT and E3:HF. Potential K_{\downarrow} was negatively correlated with ΔT_w during E1:LT, E2:HT, and E4:LT but positively correlated with ΔT_w during E3:HF. The relation between ΔQ and ΔT_w also showed a reversed pattern between E1:LT and E4:LT (positive correlations) and E2:HT (negative correlation).

Thermal sensitivity (TS), defined here as the ratio of 7-day or 5-day water temperature changes to corresponding 7-day or 5-day air temperature changes, attained a peak median value of $0.46 \text{ } ^\circ\text{C } ^\circ\text{C}^{-1}$ during E2:HT while values otherwise ranged from $0.10 \text{ } ^\circ\text{C } ^\circ\text{C}^{-1}$ to $0.17 \text{ } ^\circ\text{C } ^\circ\text{C}^{-1}$ in E1:LT, E3:HF and E4:LT (Table 1). Spatial patterns of TS were similar for E1:LT, E3:HF, and E4:LT with generally low values in northern and interior regions of the PNWNA, whereas coastal areas reached maximum values near $0.5 \text{ } ^\circ\text{C } ^\circ\text{C}^{-1}$ (Fig. 6). In contrast, TS during E2:HT was much more uniform aside from alpine waterways draining the Coast and St. Elias Mountains in BC and southeastern Alaska.

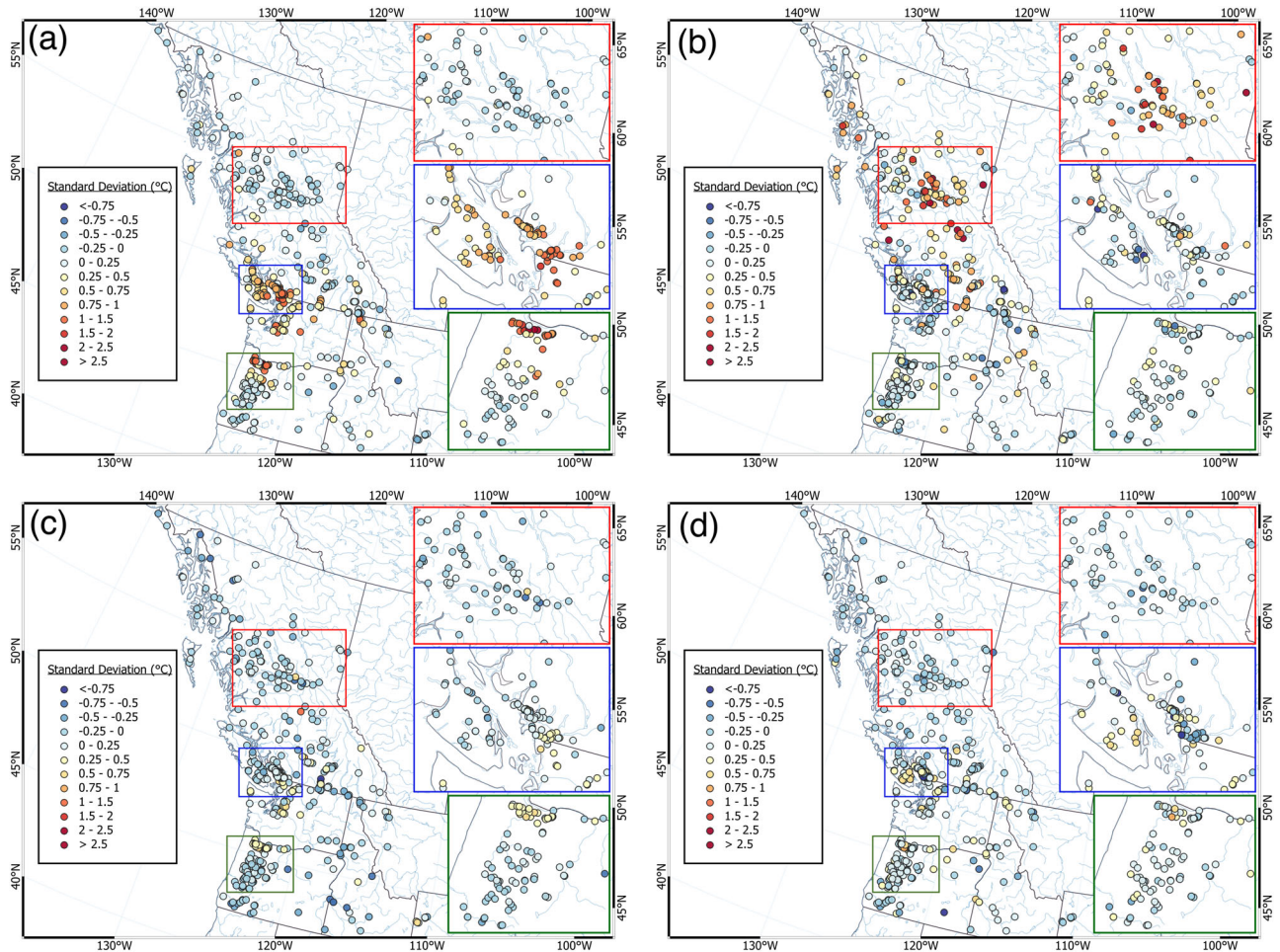


Fig. 3 | Weekly (5-day) changes in standard deviations of hourly water temperatures during four extreme hydro-meteorological events across the PNWNA in 2021. Results are shown for (a) E1:LT ($n = 440$), (b) E2:HT ($n = 506$),

(c) E3:HF ($n = 432$), and (d) E4:LT ($n = 419$). Source data to create Fig. 3 are available in Supplementary Data 4.

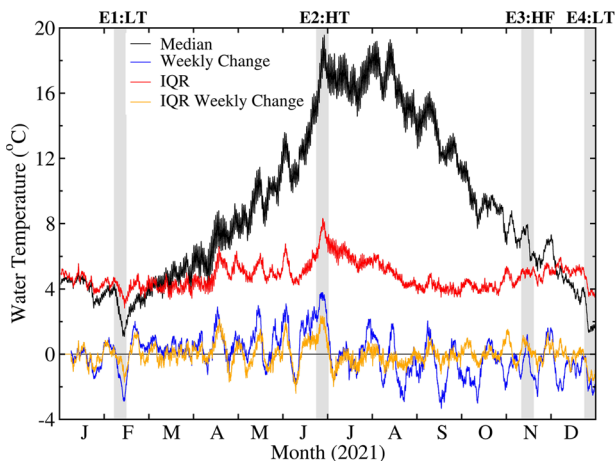


Fig. 4 | Time series of hourly median water temperature across all available sites for the PNWNA in 2021. The plot also includes the interquartile range (IQR) and weekly change (based on the median data) in water temperature and the IQR. Periods covering Events 1 (E1:LT) through 4 (E4:LT) are highlighted with gray bars. Source data to create Fig. 4 are available in Supplementary Data 5.

Synthesis of key findings

Figure 7 encapsulates the major findings of this study by ranking the responses of freshwater temperatures during four extreme

hydro-meteorological events across the PNWNA relative to the remainder of 2021. E1:LT and E4:LT induced some of the coldest water temperatures that year yielding generally low spread across sites. Weekly cooling rates were not pronounced across the northern sub-domain (owing to near-freezing conditions) but greater changes occurred in the central and southern sub-domains. During E2:HT, all six variables generally ranked in the 95th percentile or higher including mean T_w and ΔT_w . Conversely, all statistics ranked toward their central tendencies during E3:HF although ΔT_w ranked in the 90th percentile for the southern sub-domain. Based on the total number of values in the 5th and 95th percentiles, E2:HT had the most widespread impact with 17 high-ranking statistics, followed by E4:LT and E1:LT with 11 and 9, respectively with none for E3:HF. Thus, three out of the four extreme hydro-meteorological events (E1:LT, E2:HT, and E4:LT) induced atypical freshwater temperature conditions relative to the remainder of 2021 while conditions remained much more typical during E3:HF.

Discussion

Comparisons with other studies

Our study contributes to the emerging literature on the impacts of hydro-climatic extremes to river water quality including freshwater temperatures¹⁹. Most efforts thus far focused on assessing how heat waves, droughts, and climate change influence water temperatures^{8,9,13–19}. For instance, Tassone et al.⁹ recorded a doubling in the frequency of riverine heat waves during summer and fall across the US from 1996 to 2021. In response to the 2003 European summer heat wave, Piccolroaz et al.⁸ reported lowland rivers in Switzerland exhibited 60 days with river water temperatures exceeding

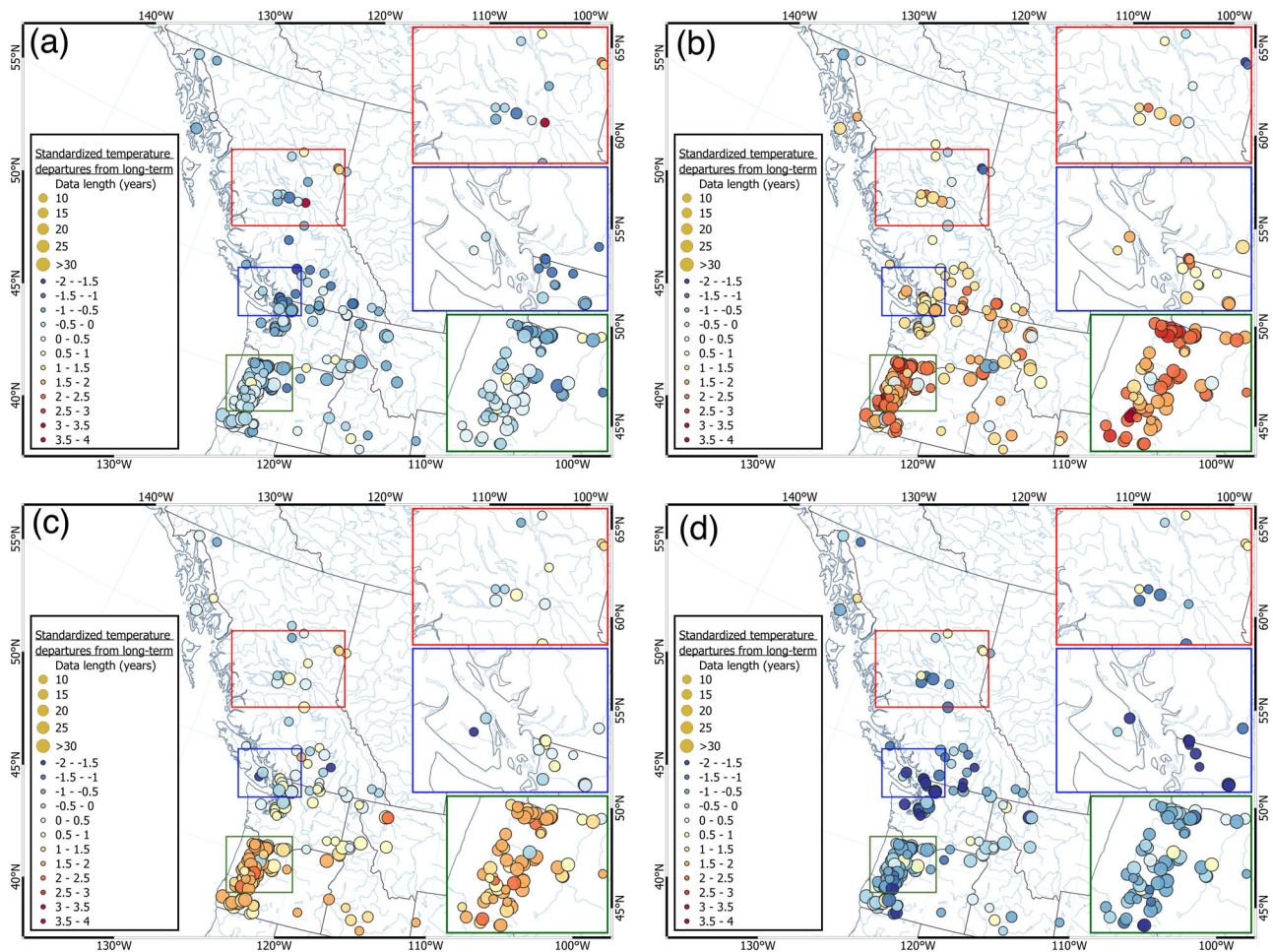


Fig. 5 | Average daily standardized anomalies of water temperatures during four extreme hydrometeorological events across the PNWNA in 2021. Results are shown for (a) E1:LT ($n = 169$), (b) E2:HT ($n = 183$), (c) E3:HF ($n = 171$), and (d)

E4:LT ($n = 162$). Circle sizes become progressively larger with increasing record lengths. Source data to create Fig. 5 are available in Supplementary Data 6.

Table 3 | Correlations between weekly or 5-day water temperature changes and terrestrial, hydrological and meteorological conditions for four extreme hydrometeorological events across the PNWNA in 2021

Event	Lat. (°N)	Lon. (°W)	Area (km ²)	Elevation (m)	T_w (°C)	ΔT_{air} (°C)	K_{\downarrow} (MJ m ⁻² day ⁻¹)	ΔQ (%)
E1:LT	0.12 440	0.03 440	0.00 313	0.04 117	-0.55 440	-0.15 440	-0.12 440	0.33 225
E2:HT	0.25 504	0.06 504	0.08 331	-0.13 116	0.37 504	0.39 504	-0.26 504	-0.44 250
E3:HF	-0.59 432	-0.11 432	-0.04 321	0.08 121	0.15 432	0.56 432	0.59 432	0.04 243
E4:LT	0.51 419	0.09 419	-0.04 311	-0.06 119	-0.68 419	-0.20 419	-0.51 419	0.36 216

Reported in the table are Spearman rank cross correlations between E1:LT, E2:HT, and E4:LT weekly and E3:HF 5-day water temperature changes (ΔT_w , °C) and the corresponding: weekly (5-day) change in WSC/USGS streamflow (ΔQ , %), weekly average potential incoming solar radiation (K_{\downarrow} , MJ m⁻² day⁻¹), weekly (5-day) change in ERA5 air temperature (ΔT_{air} , °C), weekly (5-day) average water temperature prior to each event (T_w , °C), elevation (m), catchment area (km²), longitude (Lon., °W) and latitude (Lat., °N). Bold values denote statistically significant correlations ($p < 0.05$) and numbers in italics are the sample numbers. Source data to create Table 3 are available in Supplementary Data 9.

the 90th percentile relative to 1984–2015; however, regulated and snow-fed rivers observed only muted responses to the exceptional heat wave. Steel et al.¹⁶ also reported anomalously high water temperatures in the 1813 km² Snoqualmie River Basin in Washington, US during the 2015 heat wave relative to three other years with near-normal climatic conditions; however, they observed greater sensitivity of freshwater temperatures in headwater streams rather than lowland tributaries and main stem Snoqualmie River. Based on weekly water temperature changes and thermal sensitivity during E2:HT, our results align more closely with Piccolroaz et al.⁸ with upland snow- and glacier-fed rivers observing muted or even reversed responses while their lowland counterparts showed amplified responses.

Comparatively few studies have explored freshwater temperature responses to cool season hydrometeorological extremes. Indeed, in their review of 965 published case studies, van Vliet et al.¹⁹ reported no prior efforts that investigated freshwater temperature responses to cold waves, atmospheric rivers and flooding conditions. Nonetheless, Leach and Moore²⁰ detected a 1–2 °C cooling of winter stream temperatures during rain-on-snow conditions relative to rain-on-ground conditions in a 0.11 km² watershed 60 km east of Vancouver, BC. Whitworth et al.²¹ reported a 2–3 °C cooling of water temperatures in Australia’s Goulburn River (a tributary of the Murray-Darling River) during the 2010 summer flood event but with minimal impacts during an earlier spring flood event. Cross correlations

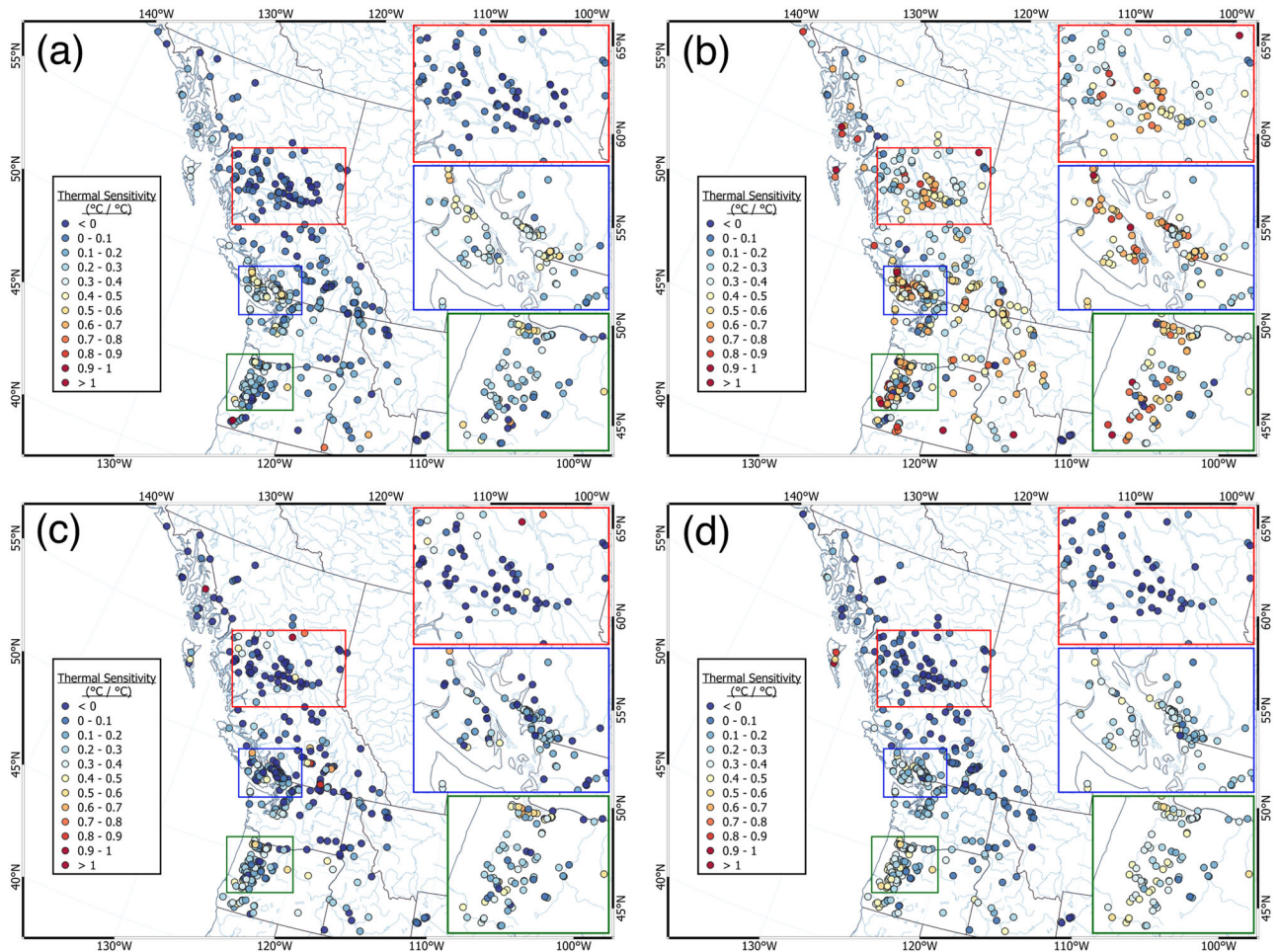


Fig. 6 | Thermal sensitivity (TS) of water temperatures during four extreme hydrometeorological events across the PNWNA in 2021. Results are shown for (a) E1:LT ($n = 420$), (b) E2:HT ($n = 491$), (c) E3:HF ($n = 410$), and (d) E4:LT ($n = 401$). Source data to create Fig. 6 are available in Supplementary Data 7.

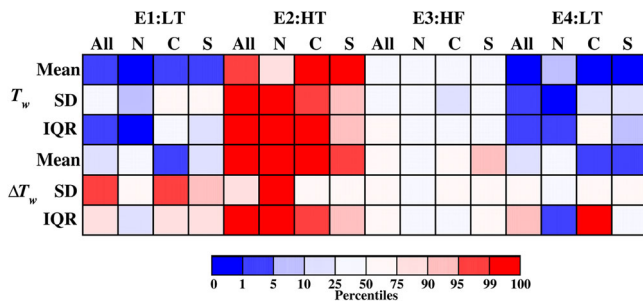


Fig. 7 | Summary of key results on the response of T_w and ΔT_w during four extreme hydrometeorological events in 2021 across the PNWNA. Results are provided for four domains of interest: the entire PNWNA (All), the northern (N), central (C), and southern (S) sub-domains. Colored boxes report the rank-based percentiles of 7-day (E1:LT, E2:HT, and E4:LT) and 5-day (E3:HF) means, standard deviations (SD) and interquartile ranges (IQR) in T_w and ΔT_w relative to all other possible 7-day or 5-day values in 2021. Here, SD represents a statistic computed at each site over time and then averaged spatially, while IQR denotes a statistic across sites that is then averaged over the duration of the event of interest. Source data to create Fig. 7 are available in Supplementary Data 8.

between weekly changes in water temperatures and discharge in the PNWNA (Table 3) suggest wintertime warming of freshwater temperatures accompanying increases in discharge while the opposite pattern occurs during summertime. Meanwhile, the flooding event of November 2021 showed no relationship between changes in 5-day water temperatures and discharge.

Thus, water temperature responses during flooding depend on the season, flood generating mechanism(s), and antecedent conditions.

Interpretation of the results

This study provides evidence that weekly freshwater temperature fluctuations of -1.2 °C to 2.7 °C can occur even when spatially averaged over a vast territory such as the PNWNA. Additionally, weekly T_w changes of -3.8 °C to $+8.5$ °C were observed at single sites during extreme hydrometeorological events. Thus, synoptic-scale meteorological systems such as frigid Arctic air masses, continental heat waves, and landfalling atmospheric rivers may induce rapid and expansive changes in T_w across the PNWNA. Nonetheless, regional patterns emerged depending on site-specific meteorological, hydrological, and geographical conditions. For instance, freshwater temperature changes during the two cold waves (E1:LT and E4:LT) and the landfalling atmospheric rivers (E3:HF) were more modest overall given the higher number of sites approaching the freezing point (possibly promoting deeper ice growth) at the time when these events occurred. As such, TS collapses to near zero in regions like the northern sub-domain during cold waves (Supplementary Table 1). Elsewhere, TS attained 0.15 – 0.35 °C °C $^{-1}$ in the central and southern domains in E1:LT, E3:HF, and E4:LT but reached ≥ 0.50 °C °C $^{-1}$ at 214 sites (42.5% of available sites) in E2:HT, implying a more robust response to ΔT_{air} during the early summer heat dome. As E2:HT occurred just a few days after the Northern Hemisphere summer solstice (20 June 2021), potential K \downarrow approached its annual peak value and was nearly uniform over the entire PNWNA, ranging from 41.1 to 41.8 MJ m $^{-2}$ day $^{-1}$ from north to south. This may explain the greater TS and more uniform response to ΔT_{air} observed during E2:HT.

While TS was generally high during E2:HT, some sites experienced low, if not negative, TS values. For instance, high-elevation streams such as Alaska's Salmon River (near Hyder) and BC's Homathko River observed $TS = -0.04\text{ }^{\circ}\text{C }^{\circ}\text{C}^{-1}$ and $-0.05\text{ }^{\circ}\text{C }^{\circ}\text{C}^{-1}$, respectively, during the heat dome as pulses of snow and glacier melt cooled freshwaters (Supplementary Fig. 6). This highlights the key role alpine snowpacks and glaciers play in buffering the impacts of summer heat waves on T_w ^{22–25}. Some heavily regulated and impounded waterways (e.g., the Clearwater in Idaho, Deschutes and Rogue rivers, both in Oregon) also showed cooling and thus negative TS values during E2:HT as water releases from upstream reservoirs ramped up, perhaps in response to increased hydroelectricity demand for climate control and/or as reservoirs approached their full capacity from seasonal snowmelt.

E3:HF showed only modest 5-day water temperature changes ($\Delta\bar{T}_w = 0.3\text{ }^{\circ}\text{C}$ at 99 sites) in the area affected by flooding (southwestern BC and northwestern Washington; see inset map on Fig. 2c and Supplementary Table 1). Nevertheless, substantial warming ($\Delta\bar{T}_w = 1.4\text{ }^{\circ}\text{C}$ at 86 sites) of streams further to the south emerged with the influx of relatively warm, subtropical air equatorward of the two landfalling atmospheric rivers (Fig. 2c and Supplementary Table 1). While T_{air} also warmed in the area directly impacted by the atmospheric rivers, abundant cloud cover, rain-on-snow, rapid snowmelt from alpine regions and high flows⁴ dampened water temperature warming. Indeed, rivers such as the Chilliwack, Coldwater, and Millstone in southwestern BC and the Skagit in northwestern Washington saw muted water temperature responses despite a surge of up to $+5\text{ }^{\circ}\text{C}$ in T_{air} relative to 6–20 November 2021 (Supplementary Fig. 7a–c, e). In contrast, the Nooksack River and an unnamed tributary to Bertrand Creek situated at lower elevations experienced up to $3\text{ }^{\circ}\text{C}$ water temperature warming during that period in response to the rise in air temperatures (Supplementary Figs. 7d, f). Representative time series of hourly water temperatures from 6 to 20 November 2021 illustrate the cooling trend in the northern sub-domain, the slight warming in the central sub-domain directly affected by flooding, and the rapid warming in the southern sub-domain during E3:HF (Supplementary Fig. 8). Thus averaging results over the entire PNWNA can mask distinct regional patterns in freshwater temperature responses during extreme hydrometeorological events. As well, this highlights the complex nature of T_w responses to landfalling atmospheric rivers and the need to expand analyses to other similar cases as atmospheric river activity peaks in September and October along BC's coast²⁶ when many Pacific salmon undertake up-river migrations and spawn²⁷.

Seasonality may also control freshwater temperature responses to extreme hydrometeorological events. For instance, the sign of Spearman rank cross correlations between ΔT_w and antecedent T_w , ΔT_{air} , and ΔQ are of opposite signs between E2:HT / E3:HF and E1:LT / E4:LT (Table 3). In relatively warm conditions (E2:HT and E3:HF), warm antecedent T_w , large increases in T_{air} , and large decreases in Q yielded amplified weekly warming of freshwater temperatures. Conversely, during relatively cool conditions (E1:LT and E4:LT), cool antecedent T_w , large decreases of T_{air} and large declines in Q accompanied amplified cooling of freshwater temperatures. Thus, statistical models relating freshwater temperature evolution as a function of meteorological, hydrological, and other environmental conditions including during extreme events should consider time of year in developing relationships between variables.

Implications of the results

Water temperature is important for several physical and chemical processes in rivers¹⁰. Water temperature variations affect a river's ability to transport sediment by controlling fluid density and kinematic fluid viscosity (both of which decrease with increasing temperature), which in turn influence a particle's settling velocity²⁸. Increased water temperature also promotes flocculation due to increased microbial activity through enhanced metabolism and the production of sticky, extracellular polymeric substances²⁹. Generally, a rise in water temperature increases the settling of sediment, thereby enhancing sedimentation on the channel bottom and reducing sediment transport for a given sediment supply. In the context of the water

temperatures observed in the PNWNA, where changes from 15 to $20\text{ }^{\circ}\text{C}$ (i.e., an increase of $5\text{ }^{\circ}\text{C}$) during the heat dome (E2:HT) were not uncommon (Figs. 1, 2), Syvitski et al.²⁸ estimates that this temperature increase could cause a $\sim 10\%$ increase in the settling velocity of a $63\text{-}\mu\text{m}$ sized particle, which denotes the boundary between fine sands and silts. The effect on particles $>63\text{-}\mu\text{m}$ would be less. Increases in settling velocity in response to warmer water temperatures are also likely to affect the transport and deposition of fine sediment-associated chemicals and contaminants, such as phosphorus, metals, persistent organic pollutants, and microplastics^{30–32}.

Changes in water temperature are also important for biological processes¹⁰. Ylla et al.^{33,34} observed during laboratory-based studies that short-term (i.e., days to weeks) increases in water temperatures by as little as $3\text{ }^{\circ}\text{C}$ resulted in changes to biofilm microbial cell numbers, respiratory activity, and metabolism. This was due to a greater decomposition of polymeric complex compounds and peptides, and a lower decomposition of lipids. This could affect river organic matter cycling and the transfer of carbon to higher trophic levels³⁴. Increased microbial activity in channel bed sediment can also alter greenhouse gas fluxes at the sediment-water interface. Comer-Warner et al.³⁵ determined that an increase in water temperature from 15 to $21\text{ }^{\circ}\text{C}$ could increase CO_2 and CH_4 fluxes from rivers to the atmosphere by 70% over previous emission estimates that have ignored channel bed sediment microbial respiration. Greenhouse gas fluxes were greatest for organic-rich, silt-dominated channel bed sediments due to greater microbial populations³⁵.

As most aquatic organisms, like invertebrates and fish, are ectotherms (i.e., they have limited physiological capacity to regulate body temperature, which is thus mainly determined by environmental temperature), water temperature will directly influence rates of all physiological processes and changes in temperature can elicit a stress response^{36,37}. However, what exactly constitutes a large and rapid temperature change to initiate a stress response in fishes and impact their fitness depends on population, life stages, and species³⁸. Among all events reported here, changes in water temperature observed during the summer heat dome (E2:HT) were the most likely to have impacted fish populations across the PNWNA to some extent. Large and rapid declines or increases in water temperature like those observed in E2:HT have been linked to changes in fish behavior (e.g., reduced foraging, increased susceptibility to predation), development, growth, and survival^{37–39}. For example, embryos of endangered white sturgeon (*Acipenser transmontanus*) in BC's Nechako River exhibit elevated mortality ($>30\%$) and suppressed metabolic rates at $21\text{ }^{\circ}\text{C}$ ⁴⁰—a threshold that was exceeded 25.6% of the time during E2:HT in the Nechako River at Vanderhoof, which overlapped the white sturgeon spawning period. In addition to the direct effects on fish, high temperature events like E2:HT cause a reduction in the amount of oxygen dissolved in water, which may further exacerbate the impacts of heat waves and sustained warming on fishes^{41–43}. As extreme hydrometeorological events influencing water temperature will increase in frequency and severity as the climate continues to warm^{44,45}, it is imperative that researchers, conservation practitioners and decision makers work together to identify, protect and create thermal refuges for freshwater fishes and other organisms⁴⁶, and to maintain important physical and chemical processes in rivers^{13,46}.

Conclusions

This study has shown that the 2021 summer heat dome across the PNWNA resulted in maximum weekly T_w approaching $28\text{ }^{\circ}\text{C}$ with weekly warming of up to $8.5\text{ }^{\circ}\text{C}$ for individual waterways. Furthermore, two extreme cold spells induced weekly cooling of up to $3.8\text{ }^{\circ}\text{C}$ in freshwater temperatures, particularly in PNWNA coastal watersheds. In contrast, the mid-November 2021 flooding caused by a pair of landfalling atmospheric rivers led generally to subdued responses in T_w for flood-affected streams as rain-on-snow and rapid snowmelt compensated for a surge in air temperatures. Thus, intense synoptic-scale events during 2021 induced widespread and rapid freshwater changes across the PNWNA although site-specific responses depended on multiple factors including geographical location, antecedent water temperatures, the magnitude and celerity of air temperature, and river discharge

changes. For instance, muted responses to the summer heat dome were observed in streams and rivers on the rising limb of the annual spring freshets as pulses of snow and glacier melt moderated T_w changes while others on the descending limb observed abrupt T_w increases. Conversely, during two cold waves, responses depended on whether antecedent T_w approached the freezing point as warmer coastal watersheds observed peak cooling of T_w . Further studies exploring the response of freshwater temperatures across a range of extreme hydrometeorological events including floods, droughts, heat, and cold waves are especially needed as climate change is anticipated to result in more frequent and intense extreme events.

Based on these results, freshwater temperatures and their changes clearly exhibited marked departures from typical conditions during the two cold waves and the heat wave; however, more typical conditions arose during the flooding event of mid-November 2021. Thus, abrupt and broadscale freshwater temperature changes are more likely to be associated with synoptic-scale high-pressure systems and their accompanying air temperature extremes. While this effort provides key information on freshwater temperature responses to three types of extreme hydro-meteorological events, further case studies would augment the range of possible responses, particularly if additional long-term records can be developed or acquired. As outlined in the Methods section, other limitations of this effort include the unknown data quality at most sites, the quality assurance process, the paucity of long-term records of freshwater temperatures (particularly in BC), and the selection of a 5-day averaging period for E3:HF but 7 days for the other three events. Efforts are therefore under way to extend the results of this study, particularly in supplementing the database of freshwater temperatures across the PNWNA and to explore other approaches for extreme event detection.

Methods

Study area

The Pacific Northwest spans a vast and diverse region of western North America⁴⁷. Here, we define the PNWNA to encompass southeastern Alaska, BC, Washington, Oregon, and parts of Idaho, Montana, and Wyoming that lie within the Columbia River Basin (Supplementary Fig. 9). This region spans from 42 to 60°N and from 110 to 140°W. The area includes major mountain chains like the Cascades, Coast, Columbia, Rocky, and St. Elias Mountains that are generally oriented north-south. Principal waterways draining to the Pacific Ocean include the Columbia, Fraser, Nass, Skeena, and Stikine Rivers, while the upper Peace River is a major system draining to the Arctic Ocean⁴⁸. While coastal rivers typically exhibit pluvial or hybrid (nival and pluvial) regimes, waterways draining mountainous and inland regions exhibit nival or glacial regimes⁴⁹. Several waterways, particularly in the Columbia River Basin, are regulated by hydroelectric dams and reservoirs; however, this is less common in the northern half of the study domain where the largest hydroelectric facilities and control structures lie within the Bridge-Seton, Nechako, and Peace River basins⁵⁰.

The PNWNA includes a wide range of climates from maritime (relatively wet and moderated temperature variability) along the Pacific Coast to continental (relatively dry, particularly to the lee of mountain chains, and amplified temperature variability) in interior regions. Sub-freezing air temperatures and abundant snowfall mark winters in high-elevation and northern regions. As such, freshwater temperatures exhibit pronounced seasonality, with peak temperatures during summer and minimum values in winter⁵¹. Nival and glacial rivers often develop an ice cover during winter and near-surface, unfrozen water remains near the freezing point. Water temperatures generally start rising once the ice cover melts and thereafter exhibit pronounced diurnal cycles.

Data

Time series of sub-daily and daily freshwater temperature (T_w) were assembled from federal and provincial agencies including the United States Geological Survey (USGS), Water Survey of Canada (WSC), Fisheries and Oceans Canada (DFO), and BC provincial monitoring sites.

These were supplemented with data from private industry (Rio Tinto, Palmer Environmental Consulting Group) plus data from UNBC networks collected by the authors in the Nechako⁵², Parsnip⁵³, and Quesnel⁵⁴ river basins. Metadata compiled for each site included collection agency, site name and identification number, coordinates, catchment area, and period of record.

Near surface meteorological conditions during the 2021 extreme hydrometeorological events were extracted from the fifth generation of the European Centre for Medium-Range Weather Forecasts (ECMWF) reanalysis (ERA5⁵⁵). Variables of interest included the hourly surface air temperatures and precipitation. To illustrate the unusual atmospheric conditions observed in the four events of interest, additional daily air temperature and precipitation data were sourced from Environment and Climate Change Canada for meteorological stations at Prince George, BC (station ID 1096453) and Hope, BC (station ID 1113542).

Site selection

Three primary criteria were used to select study sites: (1) freshwater body (river, lake, or reservoir) within the PNWNA as defined in the study area description; (2) availability of (sub-)hourly water temperature data in °C for part of, if not all of, 2021 and 2022; and (3) availability of corresponding metadata (coordinates, basin area, etc.) for the study sites. Based on these criteria, a total of 554 sites across the PNWNA were chosen for analysis (Supplementary Fig. 9 and Supplementary Data 1). Study sites comprise 536 rivers or creeks, 16 lakes, one reservoir, and one pond. A subset of 193 sites from the full database with long-term (≥ 10 years of data up to 31 December 2022) records of mean daily or hourly water temperatures were retained for additional analyses. Furthermore, hourly or daily discharge data were extracted for 270 USGS and WSC sites to explore relationships between hydrological and water temperature conditions.

Time series construction

Hourly water temperature data from 00:00 local standard time on 1 January 2021 to 23:00 local standard time on 31 December 2021 were extracted for analysis. The original time stamps for all time series were retained to reflect local standard times (Mountain, Pacific, and Alaska time zones, noting most (91%) study sites fall within the Pacific time zone). Sites where data were available at a sub-hourly scale were degraded to hourly starting at 00:00 local standard time each day. Depending on site data availability, time series of hourly water temperature data were also constructed for 2022 to assess post-E4:LT weekly changes in hydrothermal conditions. While instrument specifications were not available for most sites, water temperatures recorded within UNBC monitoring networks have an accuracy of ± 0.50 – 0.53 °C and a resolution of 0.04–0.14 °C⁵², which we expect to be representative of data accuracy for other networks.

As the quality of data retrieved from various sources was largely unknown, we developed an automated strategy to flag suspicious and potentially erroneous water temperature data. Quality assurance and quality control (QA/QC) thus followed a method adapted from Gilbert et al.⁵² and Sowder and Steel⁵⁶. Criteria used to flag potentially spurious hourly T_w data at timestep i were: (1) abrupt thermal variations of $|T_{w,i} - T_{w,i-1}| > 2.5$ °C; (2) $|T_{w,i} - T_{w,i5}^-| > 1.5$ °C where $T_{w,i5}^-$ is the rolling mean of five successive T_w data points centered on the current timestep i ; and (3) an excessive T_w diurnal range (DR) > 10 °C. All data flagged by the QA/QC criteria were then considered as missing. For criterion 3, all available data during the 24-h period (starting at 00:00 local standard time) were set as missing when DR > 10 °C. All sub-freezing T_w data that passed the QA/QC procedure were set to 0.0 °C. Temporal gaps < 24 h were in-filled through linear interpolation; otherwise, data were excluded from analysis if $> 10\%$ of values were missing for a specific period of interest. Supplementary Fig. 10 demonstrates an application of the automated QA/QC procedure in flagging suspicious hourly water temperatures for the Fraser River at Marguerite, BC during 2021.

Analyses

Analyses focused on four extreme hydrometeorological events across the PNWNA during 2021: E1:LT the cold wave of 7–13 February 2021; E2:HT the heat dome from 25 June to 1 July 2021; E3:HF the catastrophic flooding in southwestern BC and northwestern Washington during 11–15 November 2021 caused by a pair of landfalling atmospheric rivers; and E4:LT the early winter cold snap of 25–31 December 2021. To facilitate interpretation of the results, the four events of interest were assigned a dominant hydrometeorological feature of either low air temperatures (LT), high air temperatures (HT) or high flows (HF). General meteorological characteristics of the four extreme hydrometeorological events are provided in Supplementary Figs. 1–3.

Each site's 7-day (E1:LT, E2:HT, and E4:LT) or 5-day (E3:HF) average freshwater temperature was first calculated for the four events of interest when <10% of data were missing. Similar averages were computed for the 7-day or 5-day periods prior to and post events. Then, freshwater temperature differences (ΔT_w) between days during and prior to the extreme hydrometeorological events were computed. For E1:LT, E2:HT, and E4:LT, we subtracted the average hourly water temperatures of the week prior to the event from those during the event. Given the more transient nature of the shorter duration E3:HF, a similar process was taken but here focusing on the 5 days prior to and 5 days during the event. A similar approach was also employed for values of standard deviations in hourly water temperatures. Statistics (minimum, median, mean, maximum, standard deviation and interquartile range) on the event-based water temperature changes were tabulated and depicted as box and whisker plots. The Shapiro-Wilk test was applied to assess whether water temperatures were normally distributed using a probability $p = 0.05$ as the threshold⁵⁷. As all assessments indicated departures from the normal distribution (Table 2), the non-parametric Wilcoxon rank sum test was then applied to the paired values of average water temperatures prior to and during the weekly or 5-day events to assess if changes in the average were significantly ($p < 0.05$) different from zero⁵⁸. Changes in the means and standard deviations of water temperatures were also plotted spatially to reveal regional patterns during each event. An additional analysis illustrates spatial differences in freshwater temperatures between periods during and post events.

To explore the spatial synchrony of water temperature changes during Events 1–4, an additional metric was assessed. We first standardized all time series of 2021 hourly water temperature data using each site's overall mean and standard deviation. Thereafter, all possible pair-wise Spearman rank cross correlations (ρ) between standardized hourly water temperatures during the four events were computed. The median value (ρ_m) of all pair-wise cross correlations was then taken as a measure of overall spatial synchrony during Events 1–4.

To place into a longer-term context observed thermal conditions during four extreme hydrometeorological events in 2021, time series of median values and interquartile ranges of all hourly water temperatures plus weekly changes across all sites were then compiled. As well, for a subset of 193 sites with long-term water temperature records (Supplementary Data 1), standardized anomalies from daily average conditions were computed and averaged for the four events of interest. Here, standardization employed daily means and standard deviations based on each site's period of record. This provided seven values of standardized anomalies for E1:LT, E2:HT and E4:LT, and five values for E3:HF at these sites. These were then averaged for each event and reported as single values in Fig. 5. Thus, these results were restricted to days when the four extreme hydrometeorological events unfolded and excluded comparisons to other times of the year. In addition, we tracked the number of daily minimum and maximum water temperature records during each of the four events of interest for sites with records spanning at least 10 years.

Potential associations between weekly (5-day) changes in water temperatures and site metadata, hydrological and meteorological conditions were then assessed. Here, ρ values between site metadata (latitude, longitude, catchment area, and mean elevation where available), average water temperatures for the week (5 days) prior to an event, potential incoming solar

radiation ($K\downarrow$), and water temperature differences were computed. Relationships between changes in observed streamflow and water temperatures were investigated for 270 WSC and USGS sites where both quantities were available (Supplementary Data 1). Changes in streamflow were expressed as a percentage relative to the week (5 days) prior to the event. For air temperature, hourly ERA5 data at 2 m above the surface were extracted for the grid cell overlying the water temperature measurement site and averaged for the week (5 days) prior to and during the event. Weekly (5-day) changes in ERA5 air temperature were then correlated to the corresponding water temperature changes. Potential $K\downarrow$ for a flat surface was calculated at 1-min intervals using subroutines from the Catchment-based Land Surface Model⁵⁹ and time-integrated to daily radiation totals (in $\text{MJ m}^{-2} \text{day}^{-1}$) based on each site's coordinates. All ρ values were considered statistically significant when $p < 0.05$, noting that any significant correlation does not necessarily imply causation⁶⁰.

Although linear or nonlinear regressions are commonly used to assess the thermal sensitivity (TS , $^{\circ}\text{C } ^{\circ}\text{C}^{-1}$) of stream temperatures^{11,22,61–63}, we defined TS here as the ratio of changes in weekly (5-day) water temperature to the corresponding changes in air temperature at each site:

$$TS = \frac{\Delta T_w}{\Delta T_{\text{air}}} \quad (1)$$

Results for TS were plotted spatially and the median of all values (TS_m) taken as an overall measure of thermal sensitivity across the PNWNA during each event.

A final analysis synthesizes key results by ranking various statistics of T_w responses to the four extreme hydrometeorological events across the PNWNA relative to the remainder of 2021. Statistics used include the means, standard deviations and interquartile ranges of T_w and ΔT_w for all available sites which were then each assigned a nearest-rank percentile relative to all other 7-day (E1:LT, E2:HT and E4:LT) or 5-day (E3:HF) periods during 2021. Here, the T_w standard deviation was computed at each site using all available hourly T_w data for each event, and the standard deviations were then spatially averaged. Conversely, the interquartile range was computed across all available sites at each hour and then averaged over the duration of a period. Statistics for the means and standard deviations in ΔT_w represented differences between values prior to and during an event. All analyses were performed across the entire PNWNA as well as the northern, central, and southern sub-domains.

Data processing, limitations, and uncertainty

Data QA/QC and all analyses were performed using the Fortran computing language with the exception of statistics that were computed using R Studio (version 4.1.3). Spatial plots were generated in QGIS (version 3.28.5) while line, box and whisker plots were created using Grace (version 5.1.25).

Although the automated QA/QC procedure flagged on average 0.35% of the hourly T_w data across all sites during 2021, additional erroneous measurements potentially remained within the database. Similarly, some valid data may also be omitted from the database through this step. Thus, caution must be used in interpreting results for a specific site; as such, results presented herein focus on overall statistics and regional patterns during the four events of interest. Some river systems (e.g., the Columbia and Fraser Rivers) include multiple measurement sites along their main stems and tributaries thereby violating data independence. Another limitation with water temperature data used in this study is that site representativeness, instrument specifications, and set-up details are largely unknown for 522 sites outside of the UNBC networks. Nevertheless, intercomparisons of hourly water temperature data collected by different agencies in close proximity suggest they are entirely consistent with each other (Supplementary Fig. 11 and Supplementary Table 2). Thus, the quality-controlled database we have assembled is relatively homogenous and representative of temperature variations of surface waters.

Another potential shortcoming of this study is the 5-day averaging period for E3:HF but otherwise 7-day averaging periods for E1:LT, E2:HT,

and E4:LT. A 5-day averaging period was selected for E3:HF given the shorter duration of this event⁴ relative to the other three extreme hydro-meteorological events (Supplementary Figs. 3, 7). A comparison of binned freshwater temperature changes averaged over five and seven days centered on 13 November 2021, however, showed statistically indistinguishable results (Supplementary Fig. 12). Thus, to focus on the direct impacts of the two atmospheric rivers and high flows on freshwater temperatures, a 5-day period of analysis was retained for E3:HF.

A further limitation on this effort was the limited number of records used to assess departures from long-term records. This was most prevalent at Canadian sites where long-term records were particularly sparse with only one site (Fraser River at Hope, BC) having ≥ 30 years of data for the period covered by E2:HT and none for the other three events (Supplementary Fig. 13). Meanwhile, there were 37–40 sites with at least three decades of data in the US during periods spanning all four events. As such, this analysis was biased toward the southern portion of the study domain. Nevertheless, standardized anomalies for those sites with ≥ 10 years of data were representative of the subset of sites with ≥ 30 years of data (Supplementary Fig. 14).

Data availability

Water temperature data and associated metadata used in this study are available in the following publicly accessible databases: United States Geological Survey (<https://waterdata.usgs.gov/nwis>), the BC government's Real-time Water Data (<https://bcmoe-prod.aquaticinformatics.net/>) and the Pacific Data Stream (<https://pacificdatastream.ca/explore/#/dataset/4c8d3691-99e5-4fa9-ad09-da077baa37c5/?ref=search>) for Fisheries and Oceans Canada sites. Additional data collected by UNBC's Northern Hydrometeorology Group for the Nechako Watershed are available on Zenodo (<https://zenodo.org/record/6426024>) and by request to the authors for the Parsnip and Quesnel river basins. Proprietary or unpublished data for the Cheslatta, Kemano, and Nechako rivers can be requested from Rio Tinto, for Greer and Murray creeks from Palmer Environmental Consulting Group and for all Water Survey of Canada sites from the National Hydrological Services for BC. The ERA5 dataset is available online at <https://www.ecmwf.int/en/forecasts/datasets/reanalysis-datasets/era5>. All source data used to create figures and tables are available with this submission.

Code availability

Fortran and R codes developed for the analyses of water temperature and ancillary data along with a code description are available online at: <http://web.unbc.ca/~sdery/CEE.zip>.

Received: 31 December 2023; Accepted: 19 April 2024;

Published online: 01 May 2024

References

- Thompson, V. et al. The 2021 western North America heat wave among the most extreme events ever recorded globally. *Sci. Adv.* **8**, eabm6860 (2022).
- Lucarini, V., Gálfi, V. M., Messori, G. & Riboldi, J. Typicality of the 2021 Western North America summer heatwave. *Environ. Res. Lett.* **18**, 015004 (2023).
- White, R. H. et al. The unprecedented Pacific Northwest heatwave of June 2021. *Nat. Commun.* **14**, 727 (2023).
- Gillett, N. P. et al. Human influence on the 2021 British Columbia floods. *Weather Clim. Extrem.* **36**, 100441 (2022).
- Doss-Gollin, J., Farnham, D. J., Lall, U. & Modi, V. How unprecedented was the February 2021 Texas cold snap? *Environ. Res. Lett.* **16**, 064056 (2021).
- Hsu, P.-C. et al. 2021 Texas cold snap: manifestation of natural variability and a recent warming trend. *Weather Clim. Extrem.* **37**, 100476 (2022).
- Washington Post <https://www.washingtonpost.com/weather/2021/12/23/canada-northwest-cold-snow-seattle/> (2021).
- Piccolroaz, S., Toffolon, M., Robinson, C. T. & Siviglia, A. Exploring and quantifying river thermal response to heatwaves. *Water* **10**, 1098 (2018).
- Tassone, S. J. et al. Increasing heatwave frequency in streams and rivers of the United States. *Limnol. Oceanogr. Lett.* **8**, 295–304 (2023).
- Caissie, D. The thermal regime of rivers: a review. *Fresh. Biol.* **51**, 1389–1406 (2006).
- Mayer, T. D. Controls on summer stream temperature in the Pacific Northwest. *J. Hydrol.* **475**, 323–335 (2012).
- Wondzell, S. M., Diabat, M. & Haggerty, R. What matters most: are future stream temperatures more sensitive to changing air temperatures, discharge, or riparian vegetation? *J. Am. Water Resour. Assoc.* **55**, 116–132 (2019).
- Ficklin, D. L. et al. Rethinking river water temperature in a changing, human-dominated world. *Nat. Water* **1**, 125–128 (2023).
- Islam, S. U., Hay, R. W., Déry, S. J. & Booth, B. P. Modelling the impacts of climate change on riverine thermal regimes in western Canada's largest Pacific watershed. *Sci. Rep.* **9**, 11398 (2019).
- Ouellet, V. et al. River temperature research and practice: recent challenges and emerging opportunities for managing thermal habitat conditions in stream ecosystems. *Sci. Total Environ.* **736**, 139679 (2020).
- Steel, E. A. et al. Thermal landscapes in a changing climate: biological implications of water temperature patterns in an extreme year. *Can. J. Fish. Aquat. Sci.* **76**, 1740–1756 (2019).
- Wang, W. et al. The impact of extreme heat on lake warming in China. *Nat. Commun.* **15**, 70 (2024).
- White, J. C. et al. Drought impacts on river water temperature: a process-based understanding from temperate climates. *Hydrol. Process.* **37**, e14958 (2023).
- Van Vliet, M. T. H. et al. Global river water quality under climate change and hydroclimatic extremes. *Nat. Rev. Earth Environ.* **4**, 687–702 (2023).
- Leach, J. A. & Moore, R. D. Winter stream temperature in the rain-on-snow zone of the Pacific Northwest: influences of hillslope runoff and transient snow cover. *Hydrol. Earth Syst. Sci.* **18**, 819–838 (2014).
- Whitworth, K. L., Baldwin, D. S. & Kerr, J. L. Drought, floods and water quality: drivers of a severe hypoxic blackwater event in a major river system (the southern Murray-Darling Basin, Australia). *J. Hydrol.* **450–451**, 190–198 (2012).
- Moore, R. D., Nelitz, M. & Parkinson, E. Empirical modelling of maximum weekly average stream temperature in British Columbia, Canada, to support assessment of fish habitat suitability. *Can. Water Resour. J.* **38**, 135–147 (2013).
- Fellman, J. B. et al. Stream temperature response to variable glacier coverage in coastal watersheds of southeast Alaska. *Hydrol. Process.* **28**, 2062–2073 (2014).
- Luce, C. et al. Sensitivity of summer stream temperatures to climate variability in the Pacific Northwest. *Water Resour. Res.* **50**, 3428–3443 (2014).
- Du, X., Silwal, G. & Faramarzi, M. Investigating the impacts of glacier melt on stream temperature in a cold-region watershed: coupling a glacier melt model with a hydrological model. *J. Hydrol.* **605**, 127303 (2022).
- Sharma, A. R. & Déry, S. J. Variability and trends of landfalling atmospheric rivers along the Pacific Coast of northwestern North America. *Int. J. Climatol.* **40**, 544–558 (2020).
- Martins, E. G. et al. High river temperature reduces survival of sockeye salmon (*Oncorhynchus nerka*) approaching spawning grounds and exacerbates female mortality. *Can. J. Fish. Aquat. Sci.* **69**, 330–342 (2012).
- Syvitski, J., Cohen, S., Miara, A. & Best, J. River temperature and the thermal-dynamic transport of sediment. *Glob. Planet. Change* **178**, 168–183 (2019).

29. Droppo, I. G., Jeffries, D., Jaskot, C. & Backus, S. The prevalence of freshwater flocculation in cold regions: A case study from the Mackenzie River Delta, Northwest Territories, Canada. *Arctic* **51**, 155–164 (1998).
30. Owens, P. N. & Walling, D. E. The phosphorus content of fluvial sediment in rural and industrialized river basins. *Wat. Res.* **36**, 685–701 (2002).
31. Foster, I. D. L. & Charlesworth, S. M. Heavy metals in the hydrological cycle: trends and explanation. *Hydrol. Process.* **10**, 227–261 (1996).
32. Hurley, R., Woodward, J. & Rothwell, J. J. Microplastic contamination of river beds significantly reduced by catchment-wide flooding. *Nat. Geosci.* **11**, 251–257 (2018).
33. Ylla, I., Romani, A. M. & Sabater, S. Labile and recalcitrant organic matter utilization by river biofilm under increasing water temperature. *Microb. Ecol.* **64**, 593–604 (2012).
34. Ylla, I., Canhoto, C. & Romani, A. M. Effects of warming on stream biofilm organic matter use capabilities. *Microb. Ecol.* **68**, 132–145 (2014).
35. Comer-Warner, S. A. et al. Thermal sensitivity of CO₂ and CH₄ emissions varies with streambed sediment properties. *Nat. Commun.* **9**, 2803 (2018).
36. Angilletta, M. J. *Thermal Adaptation: A Theoretical and Empirical Synthesis* (Oxford Univ. Press, 2009).
37. Alfonso, S., Gesto, M. & Sadoul, B. Temperature increase and its effects on fish stress physiology in the context of global warming. *J. Fish Biol.* **98**, 1496–1508 (2021).
38. Reid, C. H. et al. An updated review of cold shock and cold stress in fish. *J. Fish Biol.* **100**, 1102–1137 (2022).
39. Donaldson, M. R., Cooke, S. J., Patterson, D. A. & Macdonald, J. S. Cold shock and fish. *J. Fish Biol.* **73**, 1491–1530 (2008).
40. Earhart, M. L. et al. Identification of upper thermal thresholds during development in the endangered Nechako white sturgeon with management implications for a regulated river. *Conserv. Physiol.* **11**, ead032 (2023).
41. Townhill, B. L., Pinnegar, J. K., Righton, D. A. & Metcalfe, J. D. Fisheries, low oxygen and climate change: how much do we really know? *J. Fish Biol.* **90**, 723–750 (2017).
42. Chapra, S. C., Camacho, L. A. & McBride, G. B. Impact of global warming on dissolved oxygen and BOD assimilative capacity of the world's rivers: modeling analysis. *Water* **13**, 2408 (2021).
43. Jane, S. F. et al. Widespread deoxygenation of temperate lakes. *Nature* **594**, 66–70 (2021).
44. Kharin, V. V., Zwiers, F. W., Zhang, X. & Wehner, M. Changes in temperature and precipitation extremes in the CMIP5 ensemble. *Clim. Change* **119**, 345–357 (2013).
45. Zhang, X. B., Zwiers, F. W., Li, G. L., Wan, H. & Cannon, A. J. Complexity in estimating past and future extreme short-duration rainfall. *Nat. Geosci.* **10**, 255–259 (2017).
46. Kurylyk, B. L., MacQuarrie, K. T. B., Linnansaari, T., Cunjak, R. A. & Curry, R. A. Preserving, augmenting, and creating cold-water thermal refugia in rivers: concepts derived from research on the Miramichi River, New Brunswick (Canada). *Ecohydrol* **8**, 1095–1108 (2015).
47. Schwantes, C. A. *The Pacific Northwest: An Interpretive History* (University of Nebraska Press, 1989).
48. Benke, A. C. & Cushing, C. E. *Rivers of North America* (Elsevier Academic Press, 2005).
49. Déry, S. J. et al. Detection of runoff timing changes in pluvial, nival, and glacial rivers of western Canada. *Water Resour. Res.* **45**, W04426 (2009).
50. Déry, S. J., Hernández-Henríquez, M. A., Stadnyk, T. A. & Troy, T. J. Vanishing weekly hydropeaking cycles in American and Canadian rivers. *Nat. Commun.* **12**, 7154 (2021).
51. Moore, R. D. Stream temperature patterns in British Columbia, Canada, based on routine spot measurements. *Can. Water Resour. J.* **31**, 41–56 (2006).
52. Gilbert, D. E., Morris, J. E., Kaveney, A. R. & Déry, S. J. Sub-hourly water temperature data collected across the Nechako Watershed, 2019–2021. *Data in Brief* **43**, 108425 (2022).
53. Martins, E. G. et al. Spatial ecology of Arctic grayling in the Parsnip Core Area PEA-F22-F-3388. Report prepared for the Fish and Wildlife Compensation Program. 73pp + 2 appendices. (2022). <https://a100.gov.bc.ca/pub/acat/public/viewReport.do?reportId=59889>
54. Petticrew, E. L. et al. The impact of a catastrophic mine tailings impoundment spill into one of North America's largest fjord lakes: Quesnel Lake, British Columbia, Canada. *Geophys. Res. Lett.* **42**, 3347–3355 (2015).
55. Hersbach, H. et al. The ERA5 global reanalysis. *Q. J. R. Meteorol. Soc.* **146**, 1999–2049 (2020).
56. Sowder, C. & Steel, E. A. A note on the collection and cleaning of water temperature data. *Water* **4**, 597–606 (2012).
57. Shapiro, S. S. & Wilk, M. B. An analysis of variance test for normality (complete samples). *Biometrika* **52**, 591–610 (1965).
58. McCuen, R. H. *Modeling Hydrologic Change: Statistical Methods* (Lewis Publishers, 2003).
59. Koster, R. D., Suarez, M. J., Ducharme, A., Stieglitz, M. & Kumar, P. A catchment-based approach to modeling land surface processes in a general circulation model. 1-Model structure. *J. Geophys. Res. Atmosph.* **105**, 809–824 (2000).
60. Johnson, S. L. Stream temperature: scaling of observations and issues for modelling. *Hydrol. Process.* **17**, 497–499 (2003).
61. Van Vliet, M. T. H., Ludwig, F., Zwolsman, J. J. G., Weedon, G. P. & Kabat, P. Global river temperatures and sensitivity to atmospheric warming and changes in river flow. *Water Resour. Res.* **47**, W02544 (2011).
62. Leach, J. A. & Moore, R. D. Empirical stream thermal sensitivities may underestimate stream temperature response to climate warming. *Water Resour. Res.* **55**, 5453–5467 (2019).
63. Ulaski, M. A., Warkentin, L., Naman, S. M. & Moore, J. W. Spatially variable effects of streamflow on water temperature and thermal sensitivity within a salmon-bearing watershed in interior British Columbia, Canada. *River Res. Appl.* **39**, 2036–2047 (2023).

Acknowledgements

Thanks to the Water Survey of Canada and its provincial partners, the BC government, Fisheries and Oceans Canada, the United States Geological Survey, Rio Tinto, and Palmer Environmental Consulting Group for providing water temperature data. Thanks to Derek Gilbert, Anna Kaveney, Jeremy Morris, Jade Reynolds, and Gracie Wilson (UNBC) for assistance with the QA/QC process, Tamar Richards-Thomas (UNBC) for ERA5 data extraction, and Aseem Sharma (BC Ministry of Forests) for creating the spatial plots. Thanks to those who assisted with the data collection effort in the Nechako Watershed: Barry Booth, Meghan Hunter-Gauthier, Derek Gilbert, Kelly Hurley, Siraj ul Islam, Anna Kaveney, Natalya Klutz, Adam MacDonald, Jeremy Morris, Jade Reynolds, Daniel Scurfield, Hadleigh Thompson, Gracie Wilson, and Spencer Woyke. Thanks to those who assisted with data collection in the Parsnip Watershed: Bryce O'Connor, Julian Napoleon, Joe Bottoms, Daniel Scurfield, Ian Clevenger, Devon Smith, David Patterson, Kendra Robinson, and Riognach Steiner. Thanks also to those who initiated and maintained the data collection effort at UNBC's Quesnel River Research Centre: Sam Albers, Todd French, and Jordan Lindgren. Funding was provided by the Natural Sciences and Engineering Research Council of Canada, Rio Tinto, and UNBC, with additional support from Environment and Climate Change Canada, Eco Canada, the Nechako Environmental Enhancement Fund, and Project Learning Tree Canada. Special thanks to the District of Vanderhoof, the Nechako Environment and Water Stewardship Society, Tatuk Lake Resort, Nadina Lake Lodge, Fisheries and Oceans Canada's Nadina River Spawning Channel, Cheslatta Carrier Nation, Stel-lat'en, Nak'azdli Whut'en, and T'azt'en First Nations for additional support. Thanks to two anonymous referees for their constructive comments that led to an improved paper.

Author contributions

S.J.D. designed the study, extracted water temperature data and constructed time series of water temperatures for all sites, developed the codes, performed the statistical and computational analyses, and drafted line and box/whisker graphs with support from E.G.M., P.N.O., and E.L.P. S.J.D. wrote the manuscript with contributions from all co-authors and all contributed to manuscript refinement and revisions.

Competing interests

The authors declare no competing interests.

Additional information

Supplementary information The online version contains supplementary material available at <https://doi.org/10.1038/s43247-024-01407-6>.

Correspondence and requests for materials should be addressed to Stephen J. Déry.

Peer review information *Communications Earth & Environment* thanks the anonymous reviewer(s) for their contribution to the peer review of this work. Primary Handling Editors: Clare Davis. A peer review file is available.

Reprints and permissions information is available at <http://www.nature.com/reprints>

Publisher's note Springer Nature remains neutral with regard to jurisdictional claims in published maps and institutional affiliations.

Open Access This article is licensed under a Creative Commons Attribution 4.0 International License, which permits use, sharing, adaptation, distribution and reproduction in any medium or format, as long as you give appropriate credit to the original author(s) and the source, provide a link to the Creative Commons licence, and indicate if changes were made. The images or other third party material in this article are included in the article's Creative Commons licence, unless indicated otherwise in a credit line to the material. If material is not included in the article's Creative Commons licence and your intended use is not permitted by statutory regulation or exceeds the permitted use, you will need to obtain permission directly from the copyright holder. To view a copy of this licence, visit <http://creativecommons.org/licenses/by/4.0/>.

© The Author(s) 2024